AMERICAN SOCIETY FOR MICROBIOLOGY | Applied and Environmental Microbiology®

BIOTECHNOLOGY

Understanding and Eliminating the Detrimental Effect of Thiamine Deficiency on the Oleaginous Yeast *Yarrowia lipolytica*

Caleb Walker,[a] Seunghyun Ryu,[a]* Richard J. Giannone,[b] Sergio Garcia,[a] Cong T. Trinh[a]

[a]Department of Chemical and Biomolecular Engineering, The University of Tennessee, Knoxville, Tennessee, USA
[b]Chemical Sciences Division, Oak Ridge National Laboratory, Oak Ridge, Tennessee, USA

Caleb Walker and Seunghyun Ryu contributed equally to this work.

ABSTRACT Thiamine is a vitamin that functions as a cofactor for key enzymes in carbon and energy metabolism in all living cells. While most plants, fungi, and bacteria can synthesize thiamine *de novo*, the oleaginous yeast *Yarrowia lipolytica* cannot. In this study, we used proteomics together with physiological characterization to elucidate key metabolic processes influenced and regulated by thiamine availability and to identify the genetic basis of thiamine auxotrophy in *Y. lipolytica*. Specifically, we found that thiamine depletion results in decreased protein abundance for the lipid biosynthesis pathway and energy metabolism (i.e., ATP synthase), leading to the negligible growth and poor sugar assimilation observed in our study. Using comparative genomics, we identified the missing 4-amino-5-hydroxymethyl-2-methylpyrimidine phosphate synthase (THI13) gene for the *de novo* thiamine biosynthesis in *Y. lipolytica* and discovered an exceptional promoter, P3, that exhibits strong activation and tight repression by low and high thiamine concentrations, respectively. Capitalizing on the strength of our thiamine-regulated promoter (P3) to express the missing gene from *Saccharomyces cerevisiae* (scTHI13), we engineered a thiamine-prototrophic *Y. lipolytica* strain. By comparing this engineered strain to the wild-type strain, we revealed the tight relationship between thiamine availability and lipid biosynthesis and demonstrated enhanced lipid production with thiamine supplementation in the engineered thiamine-prototrophic *Y. lipolytica* strain.

IMPORTANCE Thiamine plays a crucial role as an essential cofactor for enzymes involved in carbon and energy metabolism in all living cells. Thiamine deficiency has detrimental consequences for cellular health. *Yarrowia lipolytica*, a nonconventional oleaginous yeast with broad biotechnological applications, is a native thiamine auxotroph whose affected cellular metabolism is not well understood. Therefore, *Y. lipolytica* is an ideal eukaryotic host for the study of thiamine metabolism, especially because mammalian cells are also thiamine auxotrophic and thiamine deficiency is implicated in several human diseases. This study elucidates the fundamental effects of thiamine deficiency on cellular metabolism in *Y. lipolytica* and identifies genes and novel thiamine-regulated elements that eliminate thiamine auxotrophy in *Y. lipolytica*. Furthermore, the discovery of thiamine-regulated elements enables the development of thiamine biosensors with useful applications in synthetic biology and metabolic engineering.

KEYWORDS *Yarrowia lipolytica*, thiamine metabolism, thiamine auxotrophy, thiamine prototrophy, thiamine-regulated promoters, lipid production, thiamine deficiency

Thiamine (vitamin B_1) was the first B vitamin discovered. Its activated form, thiamine pyrophosphate (TPP), functions as a cofactor for key enzymes in carbon metabolism, including those in the tricarboxylic acid (TCA) (or Krebs) cycle, pentose phosphate

Citation Walker C, Ryu S, Giannone RJ, Garcia S, Trinh CT. 2020. Understanding and eliminating the detrimental effect of thiamine deficiency on the oleaginous yeast *Yarrowia lipolytica*. Appl Environ Microbiol 86:e02299-19. https://doi.org/10.1128/AEM.02299-19.

Editor Haruyuki Atomi, Kyoto University

Address correspondence to Cong T. Trinh, ctrinh@utk.edu.

* Present address: Seunghyun Ryu, CJ Research Center America, Woburn, Massachusetts, USA.

Received 8 October 2019
Accepted 5 November 2019
Accepted manuscript posted online 8 November 2019
Published 21 January 2020

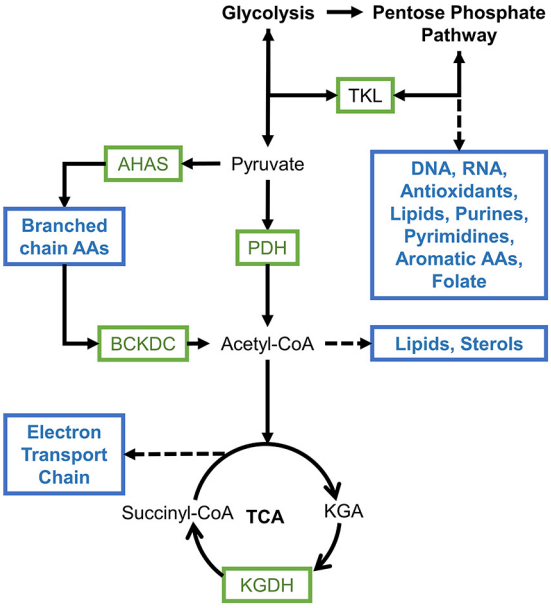

FIG 1 Metabolic map of thiamine-dependent enzymes (green) in relation to central (black) and peripheral (blue) pathways. AAs, amino acids.

pathway, and branched-chain amino acid biosynthesis pathways (Fig. 1) (1). TPP-dependent enzymes, including pyruvate dehydrogenase (PDH), α-ketoglutarate dehydrogenase (KGDH), transketolase (TKL), branched-chain α-ketoacid dehydrogenase (BCKDC), and acetolactate synthase (AHAS), are essential for maintaining cell growth and preventing metabolic stress (2–4). Specifically, PDH links glycolysis and the TCA cycle by catalyzing the conversion of pyruvate to acetyl-coenzyme A (CoA) (5, 6). KGDH, a key enzyme of the TCA cycle, converts α-ketoglutarate (KGA) to succinyl-CoA (7, 8). TKL participates in the pentose phosphate pathway by interconverting pentose sugars and glycolysis intermediates (9). The pentose phosphate pathway is critical for the production of ribose (e.g., DNA and RNA), precursor metabolites for aromatic amino acid biosynthesis pathways, and reducing equivalents (e.g., NADPH) necessary to maintain the redox balance and lipid synthesis. Hence, TKL activity is critical for DNA, RNA, protein, and lipid production while preventing oxidative stress (10, 11). AHAS and BCKDC are responsible for the synthesis and degradation, respectively, of branched-chain amino acids (i.e., valine, leucine, and isoleucine) (12, 13).

In mammals, thiamine deficiency affects the cardiovascular and nervous systems, resulting in tremors, muscle weakness, paralysis, and even death (14, 15). Thiamine deficiency can occur from inadequate intake, increased requirements, or impaired absorption of thiamine (16). Biochemical consequences of thiamine deficiency result in failure to produce ATP, increased production of acids (e.g., lactic acid), decreased production of acetylated compounds (e.g., acetylcholine), neurotransmitters (e.g., glutamate, aspartate, and aminobutyric acid), and NADH, defective RNA ribose synthesis, and failure to break down branched-chain carboxylic acids (i.e., leucine, valine, and isoleucine) (17–19).

While mammals require nutritional supplementation of thiamine from dietary sources, most bacteria, fungi, and plants can synthesize thiamine endogenously (20). One of the exceptions is the thiamine-auxotrophic oleaginous yeast *Yarrowia lipolytica*, which has recently emerged as an important industrial microbe with broad biotechnological applications due to its generally regarded as safe (GRAS) status (21), metabolic capability (22–26), and robustness (27–29). Hence, *Y. lipolytica* is an ideal eukaryotic host to study the fundamental effects of thiamine deficiency on cellular health. Currently, it is not well understood what causes failure of thiamine biosynthesis in *Y.*

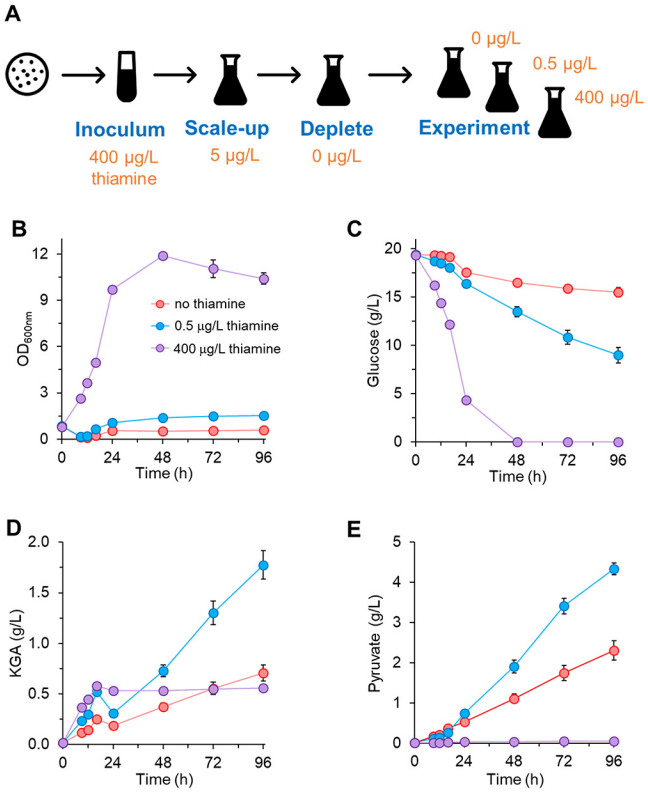

FIG 2 Growth characteristics of the thiamine-auxotrophic *Y. lipolytica* strain YlSR001 in 0 μg/liter (red), 0.5 μg/liter (blue), and 400 μg/liter (purple) thiamine. (A) Design of thiamine depletion experiments. (B) Cell growth profiles. (C) Glucose consumption profiles. (D) KGA production profiles. (E) Pyruvate production profiles.

lipolytica or how thiamine deficiency affects other processes (e.g., lipid biosynthesis and energy metabolism).

Interestingly, the auxotrophy of *Y. lipolytica* has been exploited for enhanced production of organic acids (e.g., pyruvate and KGA) by reducing the activities of PDH and KGDH under thiamine-limited conditions (30, 31). Cell growth is negatively affected by thiamine limitation and is completely prevented when thiamine is depleted from the medium. Not surprisingly, the genes for thiamine metabolism are tightly regulated by thiamine concentrations (32, 33). Numerous thiamine-regulated promoters that enable control of genetic expression through adjustments of thiamine concentrations in the culture medium have been found in yeast (34–37); however, endogenous thiamine-regulated promoters have not yet been found in *Y. lipolytica*.

In this study, we shed light on the effects of thiamine deficiency on cellular metabolism in the thiamine auxotroph *Y. lipolytica*. We identified the missing gene encoding 4-amino-5-hydroxymethyl-2-methylpyrimidine phosphate synthase (THI13) in the *de novo* thiamine biosynthesis pathway of *Y. lipolytica* and discovered a thiamine-regulated promoter, P3, that increases expression in low thiamine concentrations. By employing P3 to control the expression of scTHI13 derived from *Saccharomyces cerevisiae*, we engineered thiamine prototrophy in *Y. lipolytica*. Detailed strain characterization enabled us to elucidate the relationship between thiamine availability and lipid biosynthesis critical for enhanced lipid production in *Y. lipolytica*.

RESULTS

Effects of thiamine deficiency in *Y. lipolytica*. (i) Cell growth and organic acid production are influenced by thiamine limitation and depletion. To demonstrate the effects of thiamine limitation, we characterized the thiamine-auxotrophic *Y. lipolytica* (YlSR001) in 0, 0.5, and 400 μg/liter thiamine (Fig. 2A). Cell growth was inhibited by

limited (0.5 μg/liter thiamine) and depleted (0 μg/liter thiamine) concentrations of thiamine but was restored in medium containing high thiamine levels (400 μg/liter thiamine) (Fig. 2B). Glucose consumption profiles were closely coordinated with cell growth (Fig. 2C). Within the first 24 h, only ~2 g/liter glucose was assimilated without thiamine, while thiamine-limited cultures consumed ~3 g/liter glucose (Fig. 2C). After 24 h, growth and glucose consumption were stalled under the no-thiamine condition. In contrast, thiamine-limited cells continued to slowly utilize glucose, although growth was significantly inhibited.

Next, we characterized pyruvate and KGA production, since the enzymes converting these organic acids (PDH and KGDH, respectively) are TPP dependent. In high-thiamine medium, *Y. lipolytica* demonstrated slight KGA production (~0.5 g/liter KGA) and no pyruvate accumulation (Fig. 2D and E). We observed substantial pyruvate levels in thiamine-limited (~4 g/liter pyruvate) and thiamine-depleted (~2 g/liter pyruvate) media (Fig. 2E), indicating that PDH is unable to efficiently convert pyruvate to acetyl-CoA. Similarly, KGA accumulation was enhanced in thiamine-limited medium (2 g/liter KGA), but KGA levels in thiamine-depleted medium were comparable to those in high-thiamine medium, likely due to decreased flux from glycolysis to the TCA cycle through reduced acetyl-CoA production via PDH (Fig. 2D). Taken together, these data indicate that *Y. lipolytica* requires thiamine supplementation for cell growth and carbon assimilation but produces organic acids under thiamine-limited conditions.

(ii) The proteome with thiamine depletion reveals perturbations of critical metabolic pathways related to cell growth. Next, we investigated the proteome of the thiamine-auxotrophic *Y. lipolytica* growing in 0 or 400 μg/liter thiamine (Fig. 3A). Across two exponential time points, we identified 535 upregulated and 515 downregulated proteins (i.e., absolute $\log_2$ fold changes of >1) in response to thiamine deficiency (Fig. 3B). First, we looked at metabolic enzymes that require TPP as a cofactor, including PDH, KGDH, TKL, BCKDC, and AHAS (see Table S1 in the supplemental material). Interestingly, all proteins encoding subunits (E1 to E3) of BCKDC were upregulated with thiamine depletion (Table S1). However, none of the other TPP-requiring proteins was upregulated in medium lacking thiamine except for dihydrolipoamide dehydrogenase (E3), which serves as a subunit for BCKDC, PDH, and KGDH (Table S1).

We then mapped the 535 upregulated and 515 downregulated proteins to their respective KEGG (Kyoto Encyclopedia of Genes and Genomes) pathways (Fig. 3C). Thiamine deficiency resulted in downregulation of >55% of proteins involved in nucleotide metabolism (i.e., pyrimidine and purine metabolism) and genetic processes (i.e., ribosome and DNA replication). Without thiamine, cells also exhibited decreased protein abundance for lipid metabolism, which includes the synthesis of terpenoids (100% of proteins), steroids (75% of proteins), and glycerophospholipids (80% of proteins). In contrast, thiamine deficiency resulted in upregulation of >65% of proteins contained in carbohydrate (i.e., glycolysis and TCA cycle), tetrapyrrole, biotin, and aromatic (i.e., tryptophan and phenylalanine), branched-chain (i.e., leucine, isoleucine, and valine), and other (i.e., glycine, serine, and threonine) amino acid metabolic pathways. Thiamine deficiency also affected proteins associated with the electron transport chain (ETC), amino acid (i.e., arginine, proline, glutamate, glutamine, methionine, and cysteine) biosynthesis, and thiamine metabolic pathways.

A closer look at proteins involved in the ETC and thiamine metabolism revealed interesting features. First, thiamine-deficient cells exhibited increased protein abundances for all four complexes of the ETC but decreased protein abundance for ATP synthase, which is important for ATP generation (Fig. 3D). This phenomenon correlates with the stalled assimilation of glucose, which is ATP dependent, which is observed for cells cultured in the absence of thiamine. Second, all except one of the proteins in thiamine metabolism were differentially regulated in thiamine-sufficient versus thiamine-depleted cultures (Fig. 3E). Without thiamine, we observed increased abundance of proteins in the upper branch of thiamine biosynthesis but decreased abundance of proteins converting thiamine monophosphate into thiamine and TPP into thiamine triphosphate. The only detected protein in thiamine metabolism that was not changed by

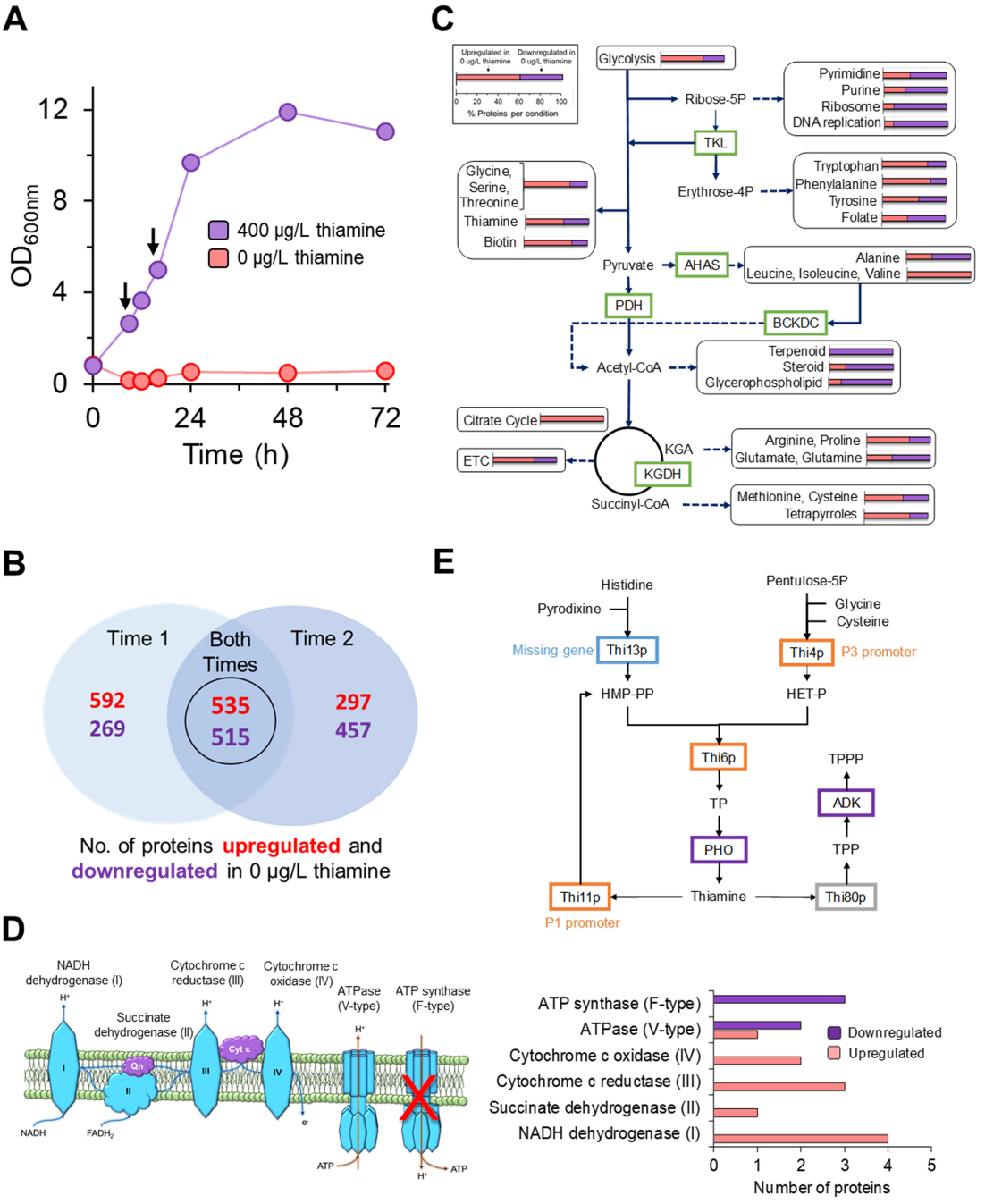

FIG 3 Proteomic analysis of the thiamine-auxotrophic *Y. lipolytica* strain YLSR001 grown in 0 μg/liter (red) and 400 μg/liter (purple) thiamine. (A) Growth profiles. Samples for proteomic analysis are indicated by arrows. (B) Venn diagram representing upregulated and downregulated proteins at the two time points. (C) Thiamine-responsive proteins in metabolic pathways. Bar graphs represent the percentages of proteins upregulated in 0 μg/liter (red) or 400 μg/liter (purple) thiamine for each pathway. (D) ETC and ATPase pathways. (E) Thiamine metabolism of *Y. lipolytica*. Enzymes are Thi4P (YALI0A09768p, thiamine thiazole synthase), Thi11p (YALI0E04224p, 4-amino-5-hydroxymethyl-2-methylpyrimidine phosphate synthase), Thi6p (YALI0C15554p, bifunctional hydroxyethylthiazole kinase/thiamine phosphate diphosphorylase), PHO (YALI0A12573p, acid phosphatase), Thi80p (YALI0E21351p, thiamine diphosphokinase), Thi13p (4-amino-5-hydroxymethyl-2-methylpyrimidine phosphate synthase), and ADK (YALI0F26521p, adenylate kinase). HET-P, hydroxyethylthiazole phosphate; HMP-PP, hydroxymethylpyrimidine pyrophosphate; TP, thiamine monophosphate; TPPP, thiamine triphosphate.

thiamine concentrations was thiamine kinase (Thi90p), which is responsible for the conversion of thiamine into its activated diphosphate form, TPP. Taken together, these data indicate that thiamine concentrations influence the regulation of thiamine metabolism, whereby thiamine deficiency severely affects central carbon metabolism and elicits in-

creased protein abundance for most carbohydrate, amino acid, and energy pathways but decreased protein abundance for lipid and nucleotide pathways (specifically, ATP synthase).

Restoring thiamine prototrophy in *Y. lipolytica*. (i) Thiamine metabolism in *Y. lipolytica* is incomplete. Next, we investigated the native thiamine metabolism of *Y. lipolytica*, to elucidate the underlying genetic deficiency causing thiamine-auxotrophic behavior. We compared the thiamine biosynthesis pathways between the well-characterized thiamine-prototrophic *Saccharomyces cerevisiae* and our thiamine-auxotrophic *Y. lipolytica*. Between the two organisms, we identified that the 4-amino-5-hydroxymethyl-2-methylpyrimidine phosphate synthase corresponding to THI13 in *S. cerevisiae* (scTHI13) is missing in *Y. lipolytica*. scTHI13 converts histidine and pyridoxine into hydroxymethylpyrimidine pyrophosphate, which is likely required for *de novo* thiamine synthesis in *Y. lipolytica* (Fig. 3E).

(ii) Constitutive expression of the missing thiamine gene does not effectively restore prototrophy. To enable the *de novo* biosynthesis of thiamine in *Y. lipolytica*, we constructed a vector to express scTHI13 under the constitutive promoter TEF, which is frequently used for genetic overexpression in *Y. lipolytica*. Unexpectedly, YlSR1005, expressing scTHI13 with the TEF promoter, restored *de novo* TPP biosynthesis only after days of adaptation in thiamine-depleted medium (Fig. S1). Additionally, cell growth varied greatly between replicates both times that this experiment was conducted (Fig. S1). Although the results were somewhat promising, we endeavored to engineer a true thiamine-prototrophic *Y. lipolytica*.

(iii) Bioinformatic analysis of thiamine-responsive genes reveals a highly regulated thiamine promoter. We hypothesized that expression of scTHI13 was weak because the constitutive TEF promoter (38, 39) is growth dependent (40, 41) and thiamine deficiency prevents cell growth. Therefore, we aimed to find a promoter responsive to thiamine deficiency. Through BLASTp and orthology analyses using the well-studied thiamine-regulated genes from *Pichia pastoris*, *S. cerevisiae*, and *Schizosaccharomyces pombe*, we identified three candidate genes that are putatively regulated by thiamine in *Y. lipolytica* (Table S2). The P1 gene (YALI0E04224g) encodes a putative thiaminase that might exhibit hydroxymethylpyrimidine kinase/phosphomethylpyrimidine kinase activity for conversion of thiamine into 4-amino-5-hydroxymethyl-2-methylpyrimidine diphosphate. The P3 gene (YALI0A09768g) encodes a putative cysteine-dependent ADP thiazole synthase that is involved in the biosynthesis of thiazole, a thiamine precursor. Thiazole synthase converts NAD^+ and glycine into ADP-5-ethyl-4-methylthiazole-2-carboxylate, a thiazole intermediate. Although the function of P2 (YALI0C14652g) has yet to be characterized, it harbors a NMT1 domain (Pfam accession no. PF09084), which is required for biosynthesis of the pyrimidine moiety of thiamine (42); hence, P2 might be thiamine regulated.

To determine whether these promoters (i.e., P1, P2, and P3) are thiamine regulated, real-time PCR (rt-PCR) was conducted to quantify mRNA levels of P1, P2, and P3 genes from YlSR001 grown in low (0.5 μg/liter) and high (500 μg/liter) concentrations of thiamine (Fig. 4A). The expression of the P1 and P3 genes was activated in low-thiamine medium but inactivated in high-thiamine medium. Remarkably, the P3 gene expression levels were substantially higher in low-thiamine medium than in high-thiamine medium. We did not observe transcriptional expression of P2 with either low or high thiamine concentrations.

We next investigated plasmid expression of these three putative thiamine-regulated promoters from *Y. lipolytica* strains harboring a humanized Renilla green fluorescent protein (hrGFP)-expressing gene under the control of the P1, P2, or P3 promoter (strain YlSR1002, YlSR1003, or YlSR1004, respectively). For controls, we also constructed the native constitutive TEF promoter and the heterologous NMT1 promoter from *S. pombe*, which has been well studied and applied as a thiamine-regulated promoter (43). The hrGFP intensity was monitored for cells grown in low (1 μg/liter) and high (10 mg/liter) concentrations of thiamine (Fig. 4B). As expected, both P1 and P3 promoters were activated under low-thiamine conditions and inactivated under high-thiamine conditions. Under low-thiamine

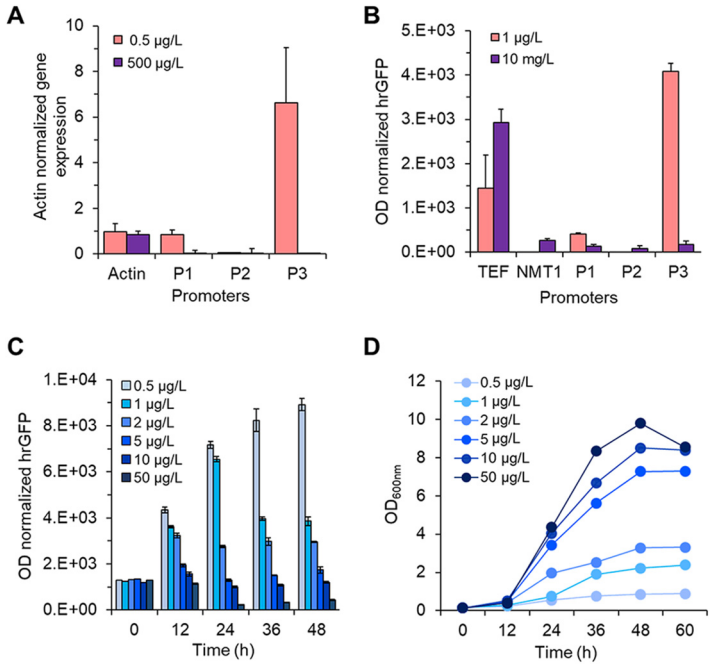

FIG 4 Thiamine-responsive promoter characterization. (A) Chromosomal gene expression of thiamine-responsive genes using rt-PCR. (B) hrGFP protein expression. (C and D) Sensitivity of the thiamine-responsive P3 promoter in the presence of increasing thiamine concentrations.

conditions, the hrGFP intensity with the P3 promoter was much higher than values with the P1 and TEF promoters (10.04 ± 0.46-fold and 2.82 ± 0.13-fold higher, respectively). Not surprisingly, the activity of the TEF promoter was much greater under high-thiamine conditions than under low-thiamine conditions. The NMT1 promoter showed no activity under low-thiamine conditions, while limited activity was observed under high-thiamine conditions, likely due to the species specificity.

We further investigated the sensitivity of the P3 promoter over a range of low thiamine concentrations (0.5 to 50 μg/liter) (Fig. 4C). Encouragingly, the P3 promoter exhibited tight regulation across all incremental thiamine concentrations. Of note, the activity of the P3 promoter was not affected by poor cell growth in low thiamine concentrations (Fig. 4D). Taken together, these data indicate that the endogenous thiamine-regulated promoters P1 and P3 can be applied to strain-engineering efforts by utilizing their response to low thiamine concentrations.

(iv) Thiamine prototrophy is restored with a thiamine-regulated promoter. To restore the *de novo* thiamine synthesis in *Y. lipolytica*, we constructed the vector pSR075 to express the missing thiamine gene, scTHI13, with the thiamine-responsive promoter P3 (yielding YlSR1006). Remarkably, this construct demonstrated robust and reproducible growth in medium lacking thiamine (Fig. 5). Cell growth and glucose uptake levels were similar with low or no added thiamine (Fig. 5A and B), but organic acid production was affected. Organic acid production under low-thiamine (0.5 μg/liter) and thiamine-depleted (0 μg/liter) conditions was diminished during the stationary phase (Fig. 5C and D). KGA accumulation manifested only under high-thiamine (400 μg/liter) conditions (Fig. 5C). Taken together, these data indicate that the thiamine-prototrophic strain created here, YlSR1006, grows reproducibly irrespective of thiamine concentrations but produces no organic acids in thiamine-limited medium.

(v) Lipid accumulation is influenced by thiamine concentrations. Finally, we investigated the relationship between thiamine availability and neutral lipid accumulation. We cultured both a thiamine-auxotrophic (wild-type) strain and our engineered thiamine-prototrophic (YlSR1006) strain with 0 μg/liter and 400 μg/liter thiamine in MpA (no nitrogen limitation) (Fig. 6A) and lipid production (nitrogen limitation, with a

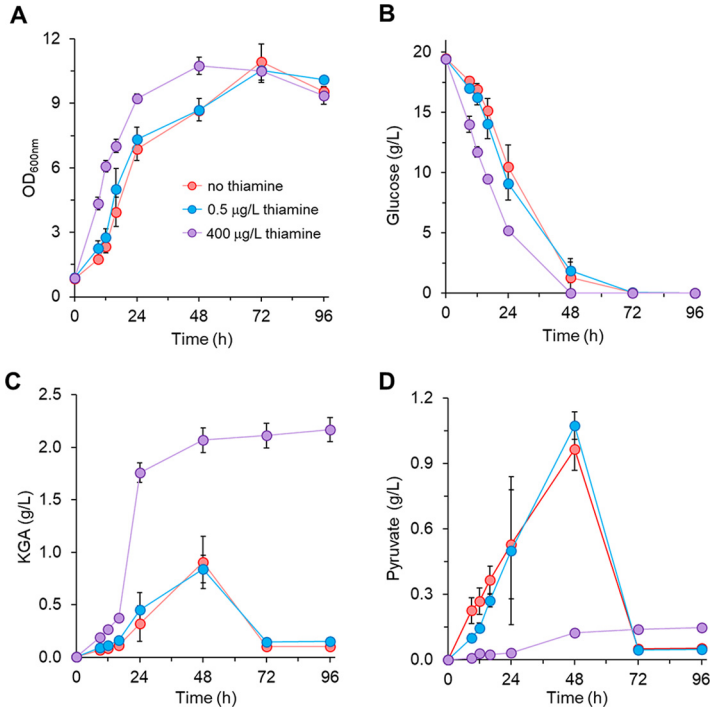

FIG 5 Expression of pP3-scTHI13 in YlSR1006 restoring *de novo* thiamine biosynthesis in *Y. lipolytica*. (A) Cell growth profiles. (B) Glucose consumption profiles. (C) KGA production profiles. (D) Pyruvate production profiles. Growth characterization was conducted in 0 μg/liter (red), 0.5 μg/liter (blue), and 400 μg/liter (purple) thiamine.

C/N ratio of 100) (Fig. 6B) media. In non-nitrogen-limited medium, YlSR1006 produced more lipid than the wild-type strain grown with 400 μg/liter thiamine supplementation (Fig. 6A). Interestingly, YlSR1006 grown without thiamine accumulated lipid levels similar to those of the wild-type strain with 400 μg/liter thiamine. Under nitrogen limitation, however, the wild-type strain and the YlSR1006 strain showed similar lipid production profiles when 400 μg/liter thiamine was supplemented in the growth medium (Fig. 6B). In thiamine-lacking medium, while no lipid accumulation was expected for the wild-type strain, YlSR1006 was able to accumulate lipids to 3.68 $\pm$ 0.22% of dry cell weight (DCW), which was ~50% less than the value for YlSR1006 supplemented with 400 μg/liter thiamine. Taken together, these data indicate that thiamine supplementation increased lipid produc-

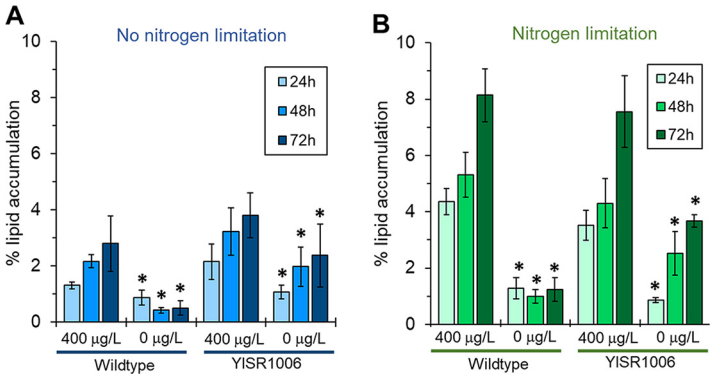

FIG 6 Lipid production influenced by thiamine availability. (A) Lipid accumulation profiles for the thiamine-auxotrophic wild-type strain YlSR001 and the thiamine-prototrophic strain YlSR1006 in 0 and 400 μg/liter thiamine. (B) Lipid accumulation profiles for thiamine-auxotrophic and thiamine-prototrophic strains in lipid production medium (C/N ratio of 100) with 0 and 400 μg/liter thiamine. Statistical significance was calculated with one-way ANOVA, with the Holm-Sidak correction, for 0 μg/liter versus 400 μg/liter thiamine for each strain. *, $P < 0.05$.

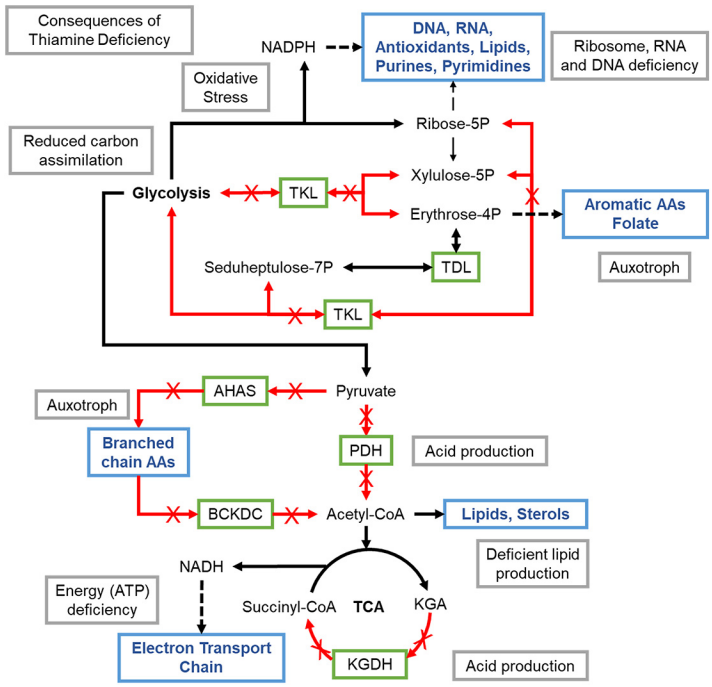

FIG 7 Comprehensive model explaining the detrimental consequences of thiamine deficiency for the metabolism and cell growth of *Y. lipolytica*. AAs, amino acids; TDL, transaldolase.

tion even for the thiamine-prototrophic strain YISR1006, demonstrating that thiamine plays a critical role in lipid biosynthesis in *Y. lipolytica*.

DISCUSSION

In this study, we observed the effects of thiamine deficiency on the growth, sugar consumption, organic acid production, and proteome of a thiamine-auxotrophic *Y. lipolytica* strain. The activated form of thiamine, TPP, is an important cofactor for enzymes involved in vital cellular functions, including energy metabolism (44), reduction of oxidative and osmotic stresses (45), and catabolism of sugars (46). Hence, the consequences of thiamine deficiency are caused by the reduced activity of TPP-dependent enzymes (i.e., PDH, KGDH, TKL, AHAS, and BCKDC), which causes growth cessation and ultimately leads to cell death. A comprehensive model that depicts the detrimental effects of thiamine deficiency on metabolism, leading to growth cessation, in *Y. lipolytica* is presented in Fig. 7.

Loss of PDH and KGDH activities results in poor growth, limited carbon assimilation, and accumulation of pyruvate and KGA (Fig. 2). Failure to metabolize pyruvate via PDH also inhibits production of acetyl-CoA, the precursor metabolite of the TCA cycle. The TCA cycle is further inhibited by reduced KGDH activity preventing the synthesis of NADH, which is required for oxidative phosphorylation (i.e., ETC). Notably, in the model yeast *S. cerevisiae*, deletion of KGDH is known to prevent respiratory growth (47), although the exact mechanism is not well established. In our study, proteomic analysis showed that thiamine-deficient cells increased protein abundance for the first four complexes of oxidative phosphorylation (i.e., NADH dehydrogenase, succinate dehydrogenase, and cytochrome c reductase/oxidase) but decreased protein abundance for ATP synthase (Fig. 3D). These new findings indicate that thiamine deficiency negatively affects respiratory energy metabolism through a malfunctioning TCA cycle via inhibition of PDH and KGDH, as demonstrated by inhibited growth and reduced sugar uptake in thiamine-depleted cells.

Y. lipolytica also decreased protein abundances for the glycerophospholipid, terpenoid backbone, and sterol biosynthesis pathways in thiamine-deficient cells (Fig. 3C). These phenomena are likely consequences of reduced PDH activity (i.e., reduced pools

of acetyl-CoA) and are likely affected by NADPH production via the pentose phosphate pathway. In the pentose phosphate pathway, TKL interconverts pentose sugars and hexose sugars, with the latter serving as glycolytic intermediates (e.g., fructose-6-phosphate and glyceraldehyde-3-phosphate). Hence, loss of TKL activity likely affects the production of ribose-5-phosphate and NADPH, which are required for synthesis of lipids, RNA, DNA, purines, pyrimidines, and antioxidants (48). Interestingly, loss of TKL activity also prevents production of erythrose-4-phosphate, impeding the synthesis of folate and aromatic amino acids (i.e., phenylalanine, tyrosine, and tryptophan), as previously observed in TKL deletion mutants of *S. cerevisiae* (49).

In our study, *Y. lipolytica* also responded to thiamine deficiency by increasing the protein abundance of enzymes involved in branched-chain α-amino acid metabolism (i.e., valine, leucine, and isoleucine). Consistent with previous studies using *S. cerevisiae* (50), deletion of BCKDC resulted in branched-chain α-amino acid-auxotrophic phenotypes. Interestingly, BCKDC was the only TPP-requiring enzyme with all three subunits upregulated in our thiamine-depleted *Y. lipolytica* cells. However, this finding might be the result of leucine supplementation in the medium, since our *Y. lipolytica* strain is leucine auxotrophic. Taken together, these data indicate that thiamine deficiency inhibited cell growth, severely limiting energy production and amino acid (i.e., aromatic and branched-chain) and lipid synthesis and ultimately leading to cell death (Fig. 7).

Despite thiamine-mediated growth inhibition, *Y. lipolytica* exhibited strong upregulation of proteins involved in thiamine metabolism in response to thiamine depletion (Fig. 3E). Interestingly, one of the enzymes upregulated in thiamine depletion, cysteine-dependent ADP thiazole synthase (YALI0A09768g), is driven by the thiamine-regulated P3 promoter. While various constitutive and inducible promoters are available for *Y. lipolytica* (51–54), the tightly regulated, thiamine-responsive P3 promoter is especially useful for strong inducible expression under low-thiamine conditions. Under optimized conditions, the activity of the P3 promoter was 2.82 ± 0.13-fold greater than that of the TEF promoter (Fig. 4B). Hence, gene overexpression using the P3 promoter is highly desirable, compared with the constitutive TEF promoter, in low thiamine concentrations. This was demonstrated by restoring thiamine prototrophy in *Y. lipolytica* using the P3 promoter (Fig. 5), while the TEF promoter was not strong enough to accomplish stable thiamine prototrophy (see Fig. S1 in the supplemental material). Overall, the P3 promoter can be used as a thiamine biosensor for applications in synthetic biology and metabolic engineering.

Surprisingly, thiamine prototrophy was restored by overexpressing a single gene, absent from the native genome of *Y. lipolytica*, for the *de novo* synthesis of thiamine (Fig. 3E; also see Fig. S1). This raises the following question: why does *Y. lipolytica* lack this gene? We hypothesize that most *Y. lipolytica* strains are isolated from thiamine-rich sources (e.g., sausage, oats, and plants) (55), while most popular yeasts, including *S. cerevisiae*, are isolated from sugar-rich sources (e.g., fruits, molasses, and sugarcane) (55). Remarkably, we observed enhanced lipid production with thiamine supplementation in both thiamine-auxotrophic and thiamine-prototrophic strains, suggesting a relationship between lipid production and thiamine availability (Fig. 6A and B). This relationship shows promise for industrial applications of neutral lipid production and establishes a novel direction for increasing lipid production in *Y. lipolytica*.

MATERIALS AND METHODS

Plasmids and strains. The plasmids and strains used in this study are presented in Table 1. Plasmid pSR005, carrying hrGFP, was constructed by the Gibson assembly method (56) with hrGFP and pSL16-CEN1-1-227 (57). The hrGFP gene was amplified from pBABE GFP using the primers hrGFP_Fwd and hrGFP_Rev (pBABE GFP [Addgene plasmid no. 10668] was a gift from William Hahn). The backbone pSL16-CEN1-1-227 was amplified with the primers pSL16_Fwd and pSL16_Rev.

Next, various promoters, including TEF (404 bp) (53), NMT1 (1,000 bp) (35), P1 (1,000 bp), P2 (1,000 bp), and P3 (1,000 bp), were inserted into pSR005 by the Gibson assembly method. The TEF, P1, P2, and P3 promoter regions were amplified from the genomic DNA of *Y. lipolytica* ATCC MYA-2613 using the primer sets P_{TEF}_Fwd/P_{TEF}_Rev, P_{P1}_Fwd/P_{P1}_Rev, P_{P2}_Fwd/P_{P2}_Rev, and P_{P3}_Fwd/P_{P3}_Rev, respectively. The NMT1 promoter region was amplified from the genomic DNA of *S. pombe* (kindly provided by Paul Dalhaimer, Department of Chemical and Biomolecular Engineering, University of Tennessee, Knoxville, TN, USA) using the P_{NMT1}_Fwd/P_{NMT1}_Rev primer set. The backbone pSR005 was amplified by using the

TABLE 1 List of plasmids and strains

Plasmid or strain	Description	Source
Plasmids		
pSL16-CEN1-1-227	pSL16-CEN1-1-227	57
pSR001	pSL16-P_{TEF}-T_{CYC1}::*leu2*	24
pSR008	pSL16-P_{TEF}-T_{CYC1}::*ura3*	25
pSR005	pSL16-hrGFP-T_{CYC1}::*leu2*	This study
pAT32y	pSL16-P_{TEF}-hrGFP-T_{CYC1}::*leu2*	This study
pSR068	pSL16-P_{NMT1}-hrGFP::*leu2*	This study
pSR071	pSL16-P_{P1}-hrGFP::*leu2*	This study
pSR072	pSL16-P_{P2}-hrGFP::*leu2*	This study
pSR073	pSL16-P_{P3}-hrGFP::*leu2*	This study
pSR074	pSL16-P_{TEF}-scTHI13-T_{CYC1}::*ura3*	This study
pSR075	pSL16-P_{P3}-scTHI13-T_{CYC1}::*ura3*	This study
Yeast strains		
YlSR001	*MATA ura3-302 leu2-270 xpr2-322 axp2-ΔNU49 XPR2::SUC2*	ATCC MYA-2613
YlSR101	YlSR001 + pSR001	24
YlSR108	YlSR001 + pSR008	25
YlSR109	YlSR001 + pAT32y	This study
YlSR1001	YlSR001 + pSR068	This study
YlSR1002	YlSR001 + pSR071	This study
YlSR1003	YlSR001 + pSR072	This study
YlSR1004	YlSR001 + pSR073	This study
YlSR1005	YlSR001 + pSR074	This study
YlSR1006	YlSR001 + pSR075	This study

pSR005_Fwd/pSR005_Rev primer set. The constructed plasmids are pAT32y, pSR068, pSR071, pSR072, and pSR073 (Table 1).

The plasmid pSR074 was constructed by assembly of (i) scTHI13, amplified from the genomic DNA of *S. cerevisiae* using the primer set scTHI13_Fwd[1]/scTHI13_Rev, and (ii) the pSR008 backbone, amplified using the primer set pSR008_Fwd/pSR008_Rev. The plasmid pSR075 was constructed by replacing the hrGFP gene with the scTHI13 gene from pSR073. The scTHI13 gene was amplified from the genomic DNA of *S. cerevisiae* by using the primer set scTHI13_Fwd[2]/scTHI13_Rev and was assembled with the P_{P3}-promoter-carrying backbone, amplified using the primer set pSR008_Fwd/pSR073_Rev.

Y. lipolytica ATCC MYA-2613, obtained from the ATCC strain collection, was used as a parent strain. The YlSR101, YlSR109, YlSR1001, and-YlSR1006 strains (Table 1) were generated by transforming the corresponding plasmids via electroporation (58). Each plasmid was transferred into *Y. lipolytica* YlSR001 via electroporation, to generate the strains used in this study. The YlSR109, YlSR1001, YlSR1002, YlSR1003, and YlSR1004 strains were confirmed by the respective promoter-binding forward primer together with hrGFP_Rev. The YlSR1005 and YlSR1006 strains were confirmed by TEF(−100)_Fwd or P3(−80)_Fwd together with the respective gene-binding reverse primer. *Escherichia coli* TOP10 was used for molecular cloning. Primers used in this study are listed in Table 2.

Media and culturing conditions. (i) Media. For *E. coli* cultures, Luria-Bertani medium containing 5 g/liter yeast extract, 10 g/liter tryptone, and 5 g/liter NaCl, with 100 mg/liter ampicillin for selection, was used. For *Y. lipolytica* characterization, MpA defined medium was used for all experiments. MpA components are as follows: 5 g/liter $(NH_4)_2SO_4$, 2 g/liter KH_2PO_4, 0.5 g/liter $MgSO_4$, 44 mg/liter $ZnSO_4{\cdot}7H_2O$, 79 mg/liter $CaCl_2{\cdot}2H_2O$, 0.8 mg/liter biotin, 100 mM HEPES buffer, 90 mM Na_2HPO_4, 10 mM NaH_2PO_4, trace elements (0.4 mg/liter $ZnSO_4{\cdot}7H_2O$, 0.04 mg/liter $CuSO_4{\cdot}5H_2O$, 0.4 mg/liter $MnSO_4{\cdot}6H_2O$, 0.2 mg/liter $Na_2MoO_4{\cdot}2H_2O$, 0.1 mg/liter KI, 0.5 mg/liter $FeSO_4{\cdot}7H_2O$, and 0.5 mg/liter H_3BO_3), 380 mg/liter leucine, 20 g/liter glucose, and various concentrations of thiamine hydrochloride. MpA medium was adjusted to pH 5.

(ii) Culturing. All experiments were conducted in a Kuhner LT-X incubator set to 28°C and 250 rpm, unless otherwise stated. Fresh colonies were inoculated overnight in 2 ml of MpA medium containing 400 μg/liter thiamine, in 15-ml culture tubes. Cultures were centrifuged and resuspended in 2 ml of water before 1 ml of this suspension was transferred into 100 ml of MpA containing 5 μg/liter thiamine for 2 days, to scale-up cultures (Fig. 2A). Next, cells were washed once with water and resuspended for 1 day in 100 ml of MpA lacking thiamine, to eliminate thiamine carryover (Fig. 2A). Finally, cells were washed twice with water before characterization experiments. All experiments were conducted in technical triplicates using 500-ml baffled flasks, unless otherwise stated.

Analytical methods. (i) Quantitative rt-PCR. *Y. lipolytica* grown in MpA medium using glucose as a carbon source, together with either low (0.5 μg/liter) or high (500 μg/liter) thiamine levels, was collected at mid-exponential phase (optical density at 600 nm [OD_{600}] of 2 to 3). Total RNA was purified by using the Qiagen RNeasy minikit (product no. 74104; Qiagen Inc., Valencia, CA, USA), and cDNA was subsequently synthesized with the QuantiTect reverse transcription kit (product no. 205311; Qiagen). To quantify mRNA expression levels for genes (e.g., actin [YALI0D08272g], P1, P2, and P3), rt-PCR assays were performed using the QuantiTect SYBR green PCR kit (product no. 204143; Qiagen) and the StepOnePlus

TABLE 2 List of primers

Promoter, gene, or plasmid	Primer	Sequence
Primers for plasmid construction		
pSL16	pSL16_Fwd	GCCTGCACGAGTGGGTGTAATCATGTAATTAGTTATGTCACGCTTAC
	pSL16_Rev	CAGGATCTGCTTGCTCACCATAGATCTGTTCGGAAATCAACGG
hrGFP	hrGFP_Fwd	AATCGGTTGAGCATCCGTTGATTTCCGAACAGATCTATGGTGAGCAAGCAGATCCTG
	hrGFP_Rev	GTAAGCGTGACATAACTAATTACATGATTACACCCACTCGTGCAGG
P_{TEF}	P_{TEF}_Fwd	CATCCGTTGATTTCCGAACAGATCTAGAGACCGGGTTGGCGGCGTATTTG
	P_{TEF}_Rev	TTCAGGATCTGCTTGCTCACCATTTTGAATGATTCTTATACTCAGAAGGAAATGCTTAAC
P_{NMT1}	P_{NMT1}_Fwd	GCATCCGTTGATTTCCGAACAGATCTTTGTATTTCAAAGGACATAATCTAAAATAATAAC
	P_{NMT1}_Rev	GGTGTTCTTCAGGATCTGCTTGCTCACCATGATTTAACAAAGCGACTATAAGTCAGAAAG
P_{P1}	P_{P1}_Fwd	GGTTGAGCATCCGTTGATTTCCGAACAGATCTTGAAGTGGGTGAGTCGCCAATTATTC
	P_{P1}_Rev	CAGGCCGGTGTTCTTCAGGATCTGCTTGCTCACCATGATCGAATTGAGTCAGCGACG
P_{P2}	P_{P2}_Fwd	CGGTTGAGCATCCGTTGATTTCCGAACAGATCTCAGGTGGTAGCAGCCCAAGACAATG
	P_{P2}_Rev	GGTGTTCTTCAGGATCTGCTTGCTCACCATGAATTGACGAACAGGTGTTTTGATG
P_{P3}	P_{P3}_Fwd	CGGTTGAGCATCCGTTGATTTCCGAACAGATCTGAGGGGTAGTCGTAAGTTTCATC
	P_{P3}_Rev	CGGTGTTCTTCAGGATCTGCTTGCTCACCATGTTAATTGTAGGTGATATAAGGGGAAG
pSR005	pSR005_Fwd	ATGGTGAGCAAGCAGATCCTG
	pSR005_Rev	AGATCTGTTCGGAAATCAACGGATGCTCAAC
scTHI13	scTHI13_Fwd[1]	CATTTCCTTCTGAGTATAAGAATCATTCAAAATGTCTACAGACAAGATCACATTTTTG
	scTHI13_Fwd[2]	CACCCTTCCCCTTATATCACCTACAATTAACATGTCTACAGACAAGATCACATTTTTG
	scTHI13_Rev	GAATGTAAGCGTGACATAACTAATTACATGATTAAGCTGGAAGAGCCAATCTCTTG
pSR008	pSR008_Fwd	TCATGTAATTAGTTATGTCACGCTTAC
	pSR008_Rev	TTTGAATGATTCTTATACTCAGAAG
pSR073	pSR073_Rev	GTTAATTGTAGGTGATATAAGGGGAAGG
Primers for checking and sequencing		
hrGFP_seq	hrGFP_Rev	CTTGCCGCAGCCCTCCATGG
TEF_seq	TEF(−100)_Fwd	CACCGTCCCCGAATTACCTTTC
P3_seq	P3(−80)_Fwd	CTGCCGTAAATCACATACTGTCGGCTG
Primers for rt-PCR		
Actin	Actin rt_Fwd	TCCAGGCCGTCCTCTCCC
	Actin rt_Ref	GGCCAGCCATATCGAGTCGCA
P1	P1 rt_Fwd	AGGACAAGGAGCCTGCCAAG
	P1 rt_Rev	GGAGGCAATGGCAGAGGCTA
P2	P2 rt_Fwd	TATGCAATCGGCCTCACCGA
	P2 rt_Rev	CTTGCCCTCCAGCTGGTCTT
P3	P3 rt_Fwd	GCTGGCTCCTGTGGTCTCTC
	P3 rt_Rev	GAACTGCTCGGCAGGCTTTC

real-time PCR system (Applied Biosystems, Foster City, CA, USA). Primers used for rt-PCR are listed in Table 2. The gene expression levels were investigated after normalization to levels of the actin housekeeping gene, as described elsewhere (25).

(ii) Promoter characterization with hrGFP. Fresh colonies of *Y. lipolytica* promoter constructs were grown overnight in 2 ml of MpA medium containing 400 μg/liter thiamine. Cultures were washed once with water and transferred overnight to 25 ml of MpA medium containing 5 μg/liter thiamine. Finally, cells were washed twice with water before being inoculated in MpA medium with various concentrations of thiamine. Incubations were performed at 400 rpm and 28°C using 96-well plates and Duetz system covers (product no. SMCR1296; Kuhner, Birsfelden, Switzerland). Sacrificial samples were collected for fluorescence measurements (excitation at 485 nm and emission at 528 nm) using a synergy HT microplate reader.

(iii) High-performance liquid chromatography. Prior to high-performance liquid chromatography (HPLC) runs, 1 ml of culture medium was filtered using a 0.2-μm filter. Metabolites, substrates, and products were quantified with a Shimadzu HPLC system equipped with UV and refractive index detectors (Shimadzu Scientific Instruments, Inc., Columbia, MD, USA) and an Aminex 87H column (Bio-Rad, Hercules, CA, USA), with a mobile phase of 10 mN H_2SO_4 at a flow rate of 0.6 ml/min. The column was maintained at 48°C (25).

(iv) Proteomic analysis. *Y. lipolytica* cells were grown in biological triplicate in 0 or 400 μg/liter thiamine. Samples were collected at two time points during the exponential growth phase and processed for liquid chromatography-tandem mass spectrometry (LC-MS/MS) analysis. Whole-cell lysates were prepared by bead beating in sodium deoxycholate (SDC) lysis buffer (4% SDC, 100 mM ammonium bicarbonate [pH 8.0]), using 0.15-mm zirconium oxide beads, and cell debris was cleared by centrifugation (21,000 $\times$ *g* for 10 min). Crude protein concentrations were measured with a NanoDrop OneC spectrophotometer (Thermo Scientific), using absorbance at 205 nm. Samples were then adjusted to 10 mM dithiothreitol and incubated at 85°C for 10 min to denature and to reduce proteins. Cysteine residues were alkylated/blocked with 30 mM iodoacetamide, followed by 20-min incubation at room temperature in the dark. Proteins (300 μg) were then transferred to a 10-kDa molecular weight cutoff (MWCO) spin

filter (Vivaspin 500; Sartorius) and digested *in situ* with proteomics-grade trypsin (Pierce), as described previously (59). The tryptic peptide solution was then filtered through the MWCO membrane by centrifugation (12,000 × *g* for 15 min) and adjusted to 1% formic acid to precipitate SDC; the SDC precipitate was removed from the peptide solution with water-saturated ethyl acetate. Peptide samples were then concentrated to dryness with a SpeedVac concentrator, resolubilized in solvent A (5% acetonitrile, 95% water, and 0.1% formic acid), and measured with a NanoDrop OneC spectrophotometer (absorbance at 205 nm), to assess tryptic peptide recovery.

Peptide samples were analyzed by automated one-dimensional LC-MS/MS analysis using a Vanquish ultra-HPLC (UHPLC) system plumbed directly in-line with a Q Exactive Plus mass spectrometer (Thermo Scientific) outfitted with a trapping column coupled to an in-house-pulled nanospray emitter. The trapping column (inner diameter, 100 μm) and the nanospray emitter (inner diameter, 75 μm) were packed with 5-μm Kinetex C_{18} reverse-phase resin (Phenomenex) to 10 cm and 30 cm, respectively. For each sample, peptides (3 μg) were loaded, desalted, separated, and analyzed across a 210-min organic gradient with the following parameters: sample injection followed by a 100% solvent A chase from 0 to 30 min (load and desalt), a linear gradient of 0% to 25% solvent B (70% acetonitrile, 30% water, and 0.1% formic acid) from 30 to 240 min (separation), a ramp to 75% solvent B from 240 to 250 min (wash), reequilibration to 100% solvent A from 250 to 260 min, and a hold at 100% solvent A from 260 to 280 min. Eluting peptides were measured and sequenced by data-dependent acquisition with the Q Exactive mass spectrometer, as described previously (59).

MS/MS spectra were searched against the *Y. lipolytica* proteome concatenated with common protein contaminants using Proteome Discover 2.2 (Thermo Scientific), employing the CharmeRT workflow (60, 61). Peptide spectrum matches (PSMs) were required to be fully tryptic with 2 miscleavages, a static modification of 57.0214 Da on cysteine (carbamidomethylated) residues, and a dynamic modification of 15.9949 Da on methionine (oxidized) residues. False-discovery rates (FDRs), as assessed by matches to decoy sequences, were initially controlled at $<$1% at both the PSM and peptide levels. FDR-controlled peptides were then quantified according to the chromatographic area under the curve and mapped to their respective proteins, and areas were summed to estimate protein-level abundance. Protein abundance distributions were then normalized across samples using InfernoRDN (62), and missing values were imputed to simulate the mass spectrometer's limit of detection using Perseus (63). Significant differences in protein abundance were calculated separately for each time point, according to the following equation:

$$\text{Fold change} = \frac{\text{WT\_0}_{t1,2} - \text{WT\_400}_{t1,2}}{\sqrt{0.25 + \Sigma\,\text{Variance}/n}}$$

Here, $\text{WT\_0}_{t1,2}$ and $\text{WT\_400}_{t1,2}$ represent $\log_2$-normalized abundances of a protein in 0 and 400 μg/liter thiamine, respectively. The denominator was used to account for errors between replicates. Variance represents the variance of protein abundance between replicates, n represents the number of replicates, and 0.25 is the pseudovariance term (64). Proteins with absolute fold changes of $>$1 were classified as upregulated or downregulated. Pathway annotations were performed with ClueGo (65), using the KEGG database (https://www.genome.jp/kegg), for proteins that were upregulated or downregulated at both time points.

(v) Bioinformatic analysis. Putative native *Y. lipolytica* thiamine-regulated promoters were identified by BLASTp (66) and orthology searches through the KEGG sequence similarity database (https://www.kegg.jp/kegg/ssdb). Reference genes used in this study were (i) *P. pastoris* hydroxymethylpyrimidine phosphate synthase *thi11* (PAS_chr4_0065) (67), (ii) *S. pombe* 4-amino-5-hydroxymethyl-2-methylpyrimidine phosphate synthase *nmt1* (GenBank accession no. NP_588347.1) (35), (iii) *S. pombe* thiamine thiazole synthase *nmt2* (GenBank accession no. NP_596642.1) (68), and (iv) *S. cerevisiae* thiamine thiazole synthase *thi4* (GenBank accession no. NP_011660.1) (69).

(vi) Lipid quantification. Thiamine-auxotrophic and thiamine-prototrophic strains were cultured with 0 and 400 μg/liter thiamine in MpA medium in triplicate, as outlined previously. Lipid samples were taken from 100-μl samples of culture broth (i.e., cells and supernatant) and incubated for 15 min at room temperature in the dark after the addition of 2 μl of 1 μg/ml boron-dipyrromethene (BODIPY) (product no. D3922; Fisher Scientific) (70), which stains neutral lipids (e.g., triacylglycerols). Lipid standards were created by dissolving 100 mg of corn oil in 20 ml of ethanol, with dilution from 1 to 0.1 mg/ml, prior to the BODIPY staining procedure. Lipids were measured using fluorescence (excitation at 485 nm and emission at 528 nm) and quantified from corn oil standards. For DCW measurements, 1 ml of culture broth was sampled from each replicate at each time point. Samples were centrifuged at maximum speed for 3 min, and the supernatant was discarded prior to sample drying at 55°C overnight. DCW was calculated by subtracting the empty tube weight from the weight of the dried cell pellet and tube. Finally, percent lipid accumulation was calculated by dividing the measured lipid concentration (in milligrams per milliliter) by the DCW (in milligrams per milliliter). Statistical significance was calculated using SigmaPlot 14 with one-way analysis of variance (ANOVA), with the Holm-Sidak correction, between 0 and 400 μg/liter thiamine for each strain.

Data availability. All raw and database-searched LC-MS/MS data pertaining to this study have been deposited into the MassIVE proteomic data repository and have been assigned the following accession numbers: MSV000084437 (MassIVE) and PXD015747 (ProteomeXchange). Data files are available at ftp://massive.ucsd.edu/MSV000084437/.

SUPPLEMENTAL MATERIAL

Supplemental material is available online only.

SUPPLEMENTAL FILE 1, PDF file, 0.4 MB.

ACKNOWLEDGMENTS

We acknowledge financial support from the DOE Biological and Environmental Research Genomic Science Program (grant DE-SC0019412) and the National Science Foundation (NSF grant 1511881).

The views, opinions, and/or findings contained in this article are those of the authors and should not be interpreted as representing the official views or policies, either expressed or implied, of the funding agencies.

REFERENCES

1. Brown GM. 1970. Biogenesis and metabolism of thiamine, 3rd ed, vol IV, p 369–378. Academic Press, New York, NY.
2. Vemuganti R, Kalluri H, Yi J-H, Bowen KK, Hazell AS. 2006. Gene expression changes in thalamus and inferior colliculus associated with inflammation, cellular stress, metabolism and structural damage in thiamine deficiency. Eur J Neurosci 23:1172–1188. https://doi.org/10.1111/j.1460-9568.2006.04651.x.
3. Bunik VI, Tylicki A, Lukashev NV. 2013. Thiamin diphosphate-dependent enzymes: from enzymology to metabolic regulation, drug design and disease models. FEBS J 280:6412–6442. https://doi.org/10.1111/febs.12512.
4. Kowalska E, Kujda M, Wolak N, Kozik A. 2012. Altered expression and activities of enzymes involved in thiamine diphosphate biosynthesis in *Saccharomyces cerevisiae* under oxidative and osmotic stress. FEMS Yeast Res 12:534–546. https://doi.org/10.1111/j.1567-1364.2012.00804.x.
5. Linn TC, Pettit FH, Reed LJ. 1969. α-Keto acid dehydrogenase complexes. X. Regulation of the activity of the pyruvate dehydrogenase complex from beef kidney mitochondria by phosphorylation and dephosphorylation. Proc Natl Acad Sci U S A 62:234–241. https://doi.org/10.1073/pnas.62.1.234.
6. Patel MS, Nemeria NS, Furey W, Jordan F. 2014. The pyruvate dehydrogenase complexes: structure-based function and regulation. J Biol Chem 289:16615–16623. https://doi.org/10.1074/jbc.R114.563148.
7. Gibson GE, Blass JP, Beal MF, Bunik V. 2005. The α-ketoglutarate-dehydrogenase complex. Mol Neurobiol 31:43–63. https://doi.org/10.1385/MN:31:1-3:043.
8. Reed LJ. 1974. Multienzyme complexes. Acc Chem Res 7:40–46. https://doi.org/10.1021/ar50074a002.
9. Schenk G, Duggleby RG, Nixon PF. 1998. Properties and functions of the thiamin diphosphate dependent enzyme transketolase. Int J Biochem Cell Biol 30:1297–1318. https://doi.org/10.1016/s1357-2725(98)00095-8.
10. Boros LG, Steinkamp MP, Fleming JC, Lee W-N, Cascante M, Neufeld EJ. 2003. Defective RNA ribose synthesis in fibroblasts from patients with thiamine-responsive megaloblastic anemia (TRMA). Blood 102:3556–3561. https://doi.org/10.1182/blood-2003-05-1537.
11. Rapala-Kozik M, Kowalska E, Ostrowska K. 2008. Modulation of thiamine metabolism in *Zea mays* seedlings under conditions of abiotic stress. J Exp Bot 59:4133–4143. https://doi.org/10.1093/jxb/ern253.
12. Pettit FH, Yeaman SJ, Reed LJ. 1978. Purification and characterization of branched chain α-keto acid dehydrogenase complex of bovine kidney. Proc Natl Acad Sci U S A 75:4881–4885. https://doi.org/10.1073/pnas.75.10.4881.
13. Ciszak EM, Korotchkina LG, Dominiak PM, Sidhu S, Patel MS. 2003. Structural basis for flip-flop action of thiamin pyrophosphate-dependent enzymes revealed by human pyruvate dehydrogenase. J Biol Chem 278:21240–21246. https://doi.org/10.1074/jbc.M300339200.
14. Williams RD, Mason HL, Smith BF, Wilder RM. 1942. Induced thiamine (vitamin B1) deficiency and the thiamine requirement of man: further observations. Arch Intern Med (Chic) 69:721–738. https://doi.org/10.1001/archinte.1942.00200170003001.
15. World Health Organization. 1999. Thiamine deficiency and its prevention and control in major emergencies. World Health Organization, Geneva, Switzerland.
16. Liu D, Ke Z, Luo J. 2017. Thiamine deficiency and neurodegeneration: the interplay among oxidative stress, endoplasmic reticulum stress, and autophagy. Mol Neurobiol 54:5440–5448. https://doi.org/10.1007/s12035-016-0079-9.
17. Bettendorff L, Goessens G, Sluse F, Wins P, Bureau M, Laschet J, Grisar T. 1995. Thiamine deficiency in cultured neuroblastoma cells: effect on mitochondrial function and peripheral benzodiazepine receptors. J Neurochem 64:2013–2021. https://doi.org/10.1046/j.1471-4159.1995.64052013.x.
18. Whitfield KC, Bourassa MW, Adamolekun B, Bergeron G, Bettendorff L, Brown KH, Cox L, Fattal-Valevski A, Fischer PR, Frank EL, Hiffler L, Hlaing LM, Jefferds ME, Kapner H, Kounnavong S, Mousavi MPS, Roth DE, Tsaloglou M-N, Wieringa F, Combs GF, Jr. 2018. Thiamine deficiency disorders: diagnosis, prevalence, and a roadmap for global control programs. Ann N Y Acad Sci 1430:3–43. https://doi.org/10.1111/nyas.13919.
19. Du Q, Wang H, Xie J. 2011. Thiamin (vitamin B1) biosynthesis and regulation: a rich source of antimicrobial drug targets? Int J Biol Sci 7:41–52. https://doi.org/10.7150/ijbs.7.41.
20. Koser SA. 1968. Vitamin requirements of bacteria and yeasts. Thomas, Springfield, IL.
21. Groenewald M, Boekhout T, Neuvéglise C, Gaillardin C, van Dijck PWM, Wyss M. 2014. *Yarrowia lipolytica*: safety assessment of an oleaginous yeast with a great industrial potential. Crit Rev Microbiol 40:187–206. https://doi.org/10.3109/1040841X.2013.770386.
22. Markham KA, Alper HS. 2018. Synthetic biology expands the industrial potential of *Yarrowia lipolytica*. Trends Biotechnol 36:1085–1095. https://doi.org/10.1016/j.tibtech.2018.05.004.
23. Hussain MS, Rodriguez GM, Gao D, Spagnuolo M, Gambill L, Blenner M. 2016. Recent advances in bioengineering of the oleaginous yeast *Yarrowia lipolytica*. Aims Bioeng 3:493–514. https://doi.org/10.3934/bioeng.2016.4.493.
24. Ryu S, Hipp J, Trinh CT. 2016. Activating and elucidating metabolism of complex sugars in *Yarrowia lipolytica*. Appl Environ Microbiol 82:1334–1345. https://doi.org/10.1128/AEM.03582-15.
25. Ryu S, Trinh CT. 2018. Understanding functional roles of native pentose-specific transporters for activating dormant pentose metabolism in *Yarrowia lipolytica*. Appl Environ Microbiol 84:e02146-17. https://doi.org/10.1128/AEM.02146-17.
26. Schwartz C, Curtis N, Löbs A-K, Wheeldon I. 2018. Multiplexed CRISPR activation of cryptic sugar metabolism enables *Yarrowia lipolytica* growth on cellobiose. Biotechnol J 13:1700584. https://doi.org/10.1002/biot.201700584.
27. Walker C, Ryu S, Trinh CT. 2019. Exceptional solvent tolerance in *Yarrowia lipolytica* is enhanced by sterols. Metab Eng 54:83–95. https://doi.org/10.1016/j.ymben.2019.03.003.
28. Ryu S, Labbé N, Trinh CT. 2015. Simultaneous saccharification and fermentation of cellulose in ionic liquid for efficient production of α-ketoglutaric acid by *Yarrowia lipolytica*. Appl Microbiol Biotechnol 99:4237–4244. https://doi.org/10.1007/s00253-015-6521-5.
29. Xu P, Qiao K, Stephanopoulos G. 2017. Engineering oxidative stress defense pathways to build a robust lipid production platform in *Yarrowia lipolytica*. Biotechnol Bioeng 114:1521–1530. https://doi.org/10.1002/bit.26285.
30. Zhou J, Zhou H, Du G, Liu L, Chen J. 2010. Screening of a thiamine-auxotrophic yeast for α-ketoglutaric acid overproduction. Lett Appl Microbiol 51:264–271. https://doi.org/10.1111/j.1472-765X.2010.02889.x.
31. Morgunov IG, Kamzolova SV, Perevoznikova OA, Shishkanova NV, Finogenova TV. 2004. Pyruvic acid production by a thiamine auxotroph of *Yarrowia lipolytica*. Process Biochem 39:1469–1474. https://doi.org/10.1016/S0032-9592(03)00259-0.
32. Li M, Petteys BJ, McClure JM, Valsakumar V, Bekiranov S, Frank EL, Smith JS. 2010. Thiamine biosynthesis in *Saccharomyces cerevisiae* is regulated by the NAD^+-dependent histone deacetylase Hst1. Mol Cell Biol 30:3329–3341. https://doi.org/10.1128/MCB.01590-09.
33. Hohmann S, Meacock PA. 1998. Thiamin metabolism and thiamin diphosphate-dependent enzymes in the yeast *Saccharomyces cerevisiae*:

genetic regulation. Biochim Biophys Acta 1385:201–219. https://doi.org/10.1016/S0167-4838(98)00069-7.
34. Landes N, Gasser B, Vorauer-Uhl K, Lhota G, Mattanovich D, Maurer M. 2016. The vitamin-sensitive promoter PTHI11 enables pre-defined autonomous induction of recombinant protein production in *Pichia pastoris*. Biotechnol Bioeng 113:2633–2643. https://doi.org/10.1002/bit.26041.
35. Moreno MB, Durán A, Ribas JC. 2000. A family of multifunctional thiamine-repressible expression vectors for fission yeast. Yeast 16:861–872. https://doi.org/10.1002/1097-0061(20000630)16:9<861::AID-YEA577>3.0.CO;2-9.
36. Basi G, Schmid E, Maundrell K. 1993. TATA box mutations in the *Schizosaccharomyces pombe nmt1* promoter affect transcription efficiency but not the transcription start point or thiamine repressibility. Gene 123:131–136. https://doi.org/10.1016/0378-1119(93)90552-e.
37. Maundrell K. 1990. *nmt1* of fission yeast: a highly transcribed gene completely repressed by thiamine. J Biol Chem 265:10857–10864.
38. Müller S, Sandal T, Kamp-Hansen P, Dalbøge H. 1998. Comparison of expression systems in the yeasts *Saccharomyces cerevisiae*, *Hansenula polymorpha*, *Kluyveromyces lactis*, *Schizosaccharomyces pombe* and *Yarrowia lipolytica*: cloning of two novel promoters from *Yarrowia lipolytica*. Yeast 14:1267–1283. https://doi.org/10.1002/(SICI)1097-0061(19981001)14:14<1267::AID-YEA327>3.0.CO;2-2.
39. Damude HG, Gillies PJ, Macool DJ, Picataggio SK, Pollak DMW, Ragghianti JJ, Xue Z, Yadav NS, Zhang H, Zhu QQ. November 2011. High eicosapentaenoic acid producing strains of *Yarrowia lipolytica*. US patent US7932077B2.
40. Scott M, Gunderson CW, Mateescu EM, Zhang Z, Hwa T. 2010. Interdependence of cell growth and gene expression: origins and consequences. Science 330:1099–1102. https://doi.org/10.1126/science.1192588.
41. Klumpp S, Zhang Z, Hwa T. 2009. Growth rate-dependent global effects on gene expression in bacteria. Cell 139:1366–1375. https://doi.org/10.1016/j.cell.2009.12.001.
42. Rodríguez-Navarro S, Llorente B, Rodríguez-Manzaneque MT, Ramne A, Uber G, Marchesan D, Dujon B, Herrero E, Sunnerhagen P, Pérez-Ortín JE. 2002. Functional analysis of yeast gene families involved in metabolism of vitamins B_1 and B_6. Yeast 19:1261–1276. https://doi.org/10.1002/yea.916.
43. Maundrell K. 1993. Thiamine-repressible expression vectors pREP and pRIP for fission yeast. Gene 123:127–130. https://doi.org/10.1016/0378-1119(93)90551-d.
44. Lonsdale D. 2006. A review of the biochemistry, metabolism and clinical benefits of thiamin(e) and its derivatives. Evid Based Complement Alternat Med 3:49–59. https://doi.org/10.1093/ecam/nek009.
45. Wolak N, Kowalska E, Kozik A, Rapala-Kozik M. 2014. Thiamine increases the resistance of baker's yeast *Saccharomyces cerevisiae* against oxidative, osmotic and thermal stress, through mechanisms partly independent of thiamine diphosphate-bound enzymes. FEMS Yeast Res 14:1249–1262. https://doi.org/10.1111/1567-1364.12218.
46. Singleton CK, Martin PR. 2001. Molecular mechanisms of thiamine utilization. Curr Mol Med 1:197–207. https://doi.org/10.2174/1566524013363870.
47. Dimmer KS, Fritz S, Fuchs F, Messerschmitt M, Weinbach N, Neupert W, Westermann B. 2002. Genetic basis of mitochondrial function and morphology in *Saccharomyces cerevisiae*. Mol Biol Cell 13:847–853. https://doi.org/10.1091/mbc.01-12-0588.
48. Fattal-Valevski A. 2011. Thiamine (vitamin B_1). J Evid Based Complement Alternat Med 16:12–20. https://doi.org/10.1177/1533210110392941.
49. Sundström M, Lindqvist Y, Schneider G, Hellman U, Ronne H. 1993. Yeast TKL1 gene encodes a transketolase that is required for efficient glycolysis and biosynthesis of aromatic amino acids. J Biol Chem 268:24346–24352.
50. Kispal G, Steiner H, Court DA, Rolinski B, Lill R. 1996. Mitochondrial and cytosolic branched-chain amino acid transaminases from yeast, homologs of the *myc* oncogene-regulated Eca39 protein. J Biol Chem 271:24458–24464. https://doi.org/10.1074/jbc.271.40.24458.
51. Shabbir Hussain M, Gambill L, Smith S, Blenner MA. 2016. Engineering promoter architecture in oleaginous yeast *Yarrowia lipolytica*. ACS Synth Biol 5:213–223. https://doi.org/10.1021/acssynbio.5b00100.
52. Trassaert M, Vandermies M, Carly F, Denies O, Thomas S, Fickers P, Nicaud J-M. 2017. New inducible promoter for gene expression and synthetic biology in *Yarrowia lipolytica*. Microb Cell Fact 16:141. https://doi.org/10.1186/s12934-017-0755-0.
53. Blazeck J, Liu L, Redden H, Alper H. 2011. Tuning gene expression in *Yarrowia lipolytica* by a hybrid promoter approach. Appl Environ Microbiol 77:7905–7914. https://doi.org/10.1128/AEM.05763-11.
54. Nicaud J-M, Madzak C, van den Broek P, Gysler C, Duboc P, Niederberger P, Gaillardin C. 2002. Protein expression and secretion in the yeast *Yarrowia lipolytica*. FEMS Yeast Res 2:371–379. https://doi.org/10.1016/S1567-1356(02)00082-X.
55. Tikka C, Osuru HP, Atluri N, Raghavulu PCV, Yellapu NK, Mannur IS, Prasad UV, Aluru S, K NV, Bhaskar M. 2013. Isolation and characterization of ethanol tolerant yeast strains. Bioinformation 9:421–425. https://doi.org/10.6026/97320630009421.
56. Gibson DG, Young L, Chuang R-Y, Venter JC, Hutchison CA, Smith HO. 2009. Enzymatic assembly of DNA molecules up to several hundred kilobases. Nat Methods 6:343–345. https://doi.org/10.1038/nmeth.1318.
57. Yamane T, Sakai H, Nagahama K, Ogawa T, Matsuoka M. 2008. Dissection of centromeric DNA from yeast *Yarrowia lipolytica* and identification of protein-binding site required for plasmid transmission. J Biosci Bioeng 105:571–578. https://doi.org/10.1263/jbb.105.571.
58. Wang JH, Hung WP, Tsai SH. 2011. High efficiency transformation by electroporation of *Yarrowia lipolytica*. J Microbiol 49:469–472. https://doi.org/10.1007/s12275-011-0433-6.
59. Clarkson SM, Giannone RJ, Kridelbaugh DM, Elkins JG, Guss AM, Michener JK. 2017. Construction and optimization of a heterologous pathway for protocatechuate catabolism in *Escherichia coli* enables bioconversion of model aromatic compounds. Appl Environ Microbiol 83:e01313-17. https://doi.org/10.1128/AEM.01313-17.
60. Villalobos Solis MI, Giannone RJ, Hettich RL, Abraham PE. 2019. Exploiting the dynamic relationship between peptide separation quality and peptide coisolation in a multiple-peptide matches-per-spectrum approach offers a strategy to optimize bottom-up proteomics throughput and depth. Anal Chem 91:7273–7279. https://doi.org/10.1021/acs.analchem.9b00819.
61. Dorfer V, Maltsev S, Winkler S, Mechtler K. 2018. CharmeRT: boosting peptide identifications by chimeric spectra identification and retention time prediction. J Proteome Res 17:2581–2589. https://doi.org/10.1021/acs.jproteome.7b00836.
62. Taverner T, Karpievitch YV, Polpitiya AD, Brown JN, Dabney AR, Anderson GA, Smith RD. 2012. DanteR: an extensible R-based tool for quantitative analysis of -omics data. Bioinformatics 28:2404–2406. https://doi.org/10.1093/bioinformatics/bts449.
63. Tyanova S, Temu T, Sinitcyn P, Carlson A, Hein MY, Geiger T, Mann M, Cox J. 2016. The Perseus computational platform for comprehensive analysis of (prote)omics data. Nat Methods 13:731. https://doi.org/10.1038/nmeth.3901.
64. Mukhopadhyay A, He Z, Alm EJ, Arkin AP, Baidoo EE, Borglin SC, Chen W, Hazen TC, He Q, Holman H-Y, Huang K, Huang R, Joyner DC, Katz N, Keller M, Oeller P, Redding A, Sun J, Wall J, Wei J, Yang Z, Yen H-C, Zhou J, Keasling JD. 2006. Salt stress in *Desulfovibrio vulgaris*: an integrated genomics approach. J Bacteriol 188:4068–4078. https://doi.org/10.1128/JB.01921-05.
65. Bindea G, Mlecnik B, Hackl H, Charoentong P, Tosolini M, Kirilovsky A, Fridman W-H, Pagès F, Trajanoski Z, Galon J. 2009. ClueGO: a Cytoscape plug-in to decipher functionally grouped gene ontology and pathway annotation networks. Bioinformatics 25:1091–1093. https://doi.org/10.1093/bioinformatics/btp101.
66. Altschul SF, Madden TL, Schaffer AA, Zhang J, Zhang Z, Miller W, Lipman DJ. 1997. Gapped BLAST and PSI-BLAST: a new generation of protein database search programs. Nucleic Acids Res 25:3389–3402. https://doi.org/10.1093/nar/25.17.3389.
67. Delic M, Mattanovich D, Gasser B. 2013. Repressible promoters: a novel tool to generate conditional mutants in *Pichia pastoris*. Microb Cell Fact 12:6. https://doi.org/10.1186/1475-2859-12-6.
68. Manetti AG, Rosetto M, Maundrell KG. 1994. *nmt2* of fission yeast: a second thiamine-repressible gene co-ordinately regulated with *nmt1*. Yeast 10:1075–1082. https://doi.org/10.1002/yea.320100809.
69. Praekelt UM, Byrne KL, Meacock PA. 1994. Regulation of THI4 (MOL1), a thiamine-biosynthetic gene of *Saccharomyces cerevisiae*. Yeast 10:481–490. https://doi.org/10.1002/yea.320100407.
70. Klapper M, Ehmke M, Palgunow D, Böhme M, Matthäus C, Bergner G, Dietzek B, Popp J, Döring F. 2011. Fluorescence-based fixative and vital staining of lipid droplets in *Caenorhabditis elegans* reveal fat stores using microscopy and flow cytometry approaches. J Lipid Res 52:1281–1293. https://doi.org/10.1194/jlr.D011940.